COMPARISONS OF WIND TUNNEL AND FULL-SCALE BUILDING SURFACE PRESSURES WITH EMPHASIS ON PEAKS

W. A. DALGLIESH, J. T. TEMPLIN and
K. R. COOPER
National Research Council of Canada, Ottawa, Ontario, Canada

SUMMARY

Full-scale pressure coefficients obtained from a 57-storey building in Toronto and wind tunnel results from tests in the 9 m by 9 m wind tunnel at the National Research Council of Canada are compared and demonstrate good agreement where sufficient full-scale data exist. A method of treating peak pressures is proposed based on the fit of an exponential distribution to a population of "significant independent events," called pressure spikes. This distribution provides a good fit to both full-scale and wind tunnel results, which generally agree.

INTRODUCTION

An important application of wind tunnel testing is the provision of the surface pressure loads that are required for the design of cladding of tall buildings. There is a growing confidence that careful simulation of the flow-field and nearby structures will produce information that accurately reflects the full-scale situation. Recent comparisons of model and full-scale pressure measurements have shown that this can be said about the mean value and the standard deviation of surface pressure fluctuations[1, 2, 3], but not with equal confidence about the peak pressures because it is difficult to find a representative value[4] and because unusually high peaks, occasionally found in full scale[5], might not be reproduced or detected at model scale.

This paper explores two subjects:

(1) The difficulties in obtaining full-scale pressure measurements for the comparison with wind tunnel findings are discussed based on recent full-scale observations and the results of a new wind tunnel test. The full-scale measurements were made on the Commerce Court building in downtown Toronto; the model experiments were performed on a 1:200 scale model mounted in the 9 m by 9 m wind tunnel of the National Aeronautical Establishment in Ottawa. The discussion emphasizes the variability in full-scale pressure measurements that does not arise in the wind tunnel.

(2) An approach to the study of peak pressures is introduced based on fitting an exponential distribution to a population of "significant independent events" called spikes. A discussion of time scaling is presented which enables comparison of model and full-scale observations.

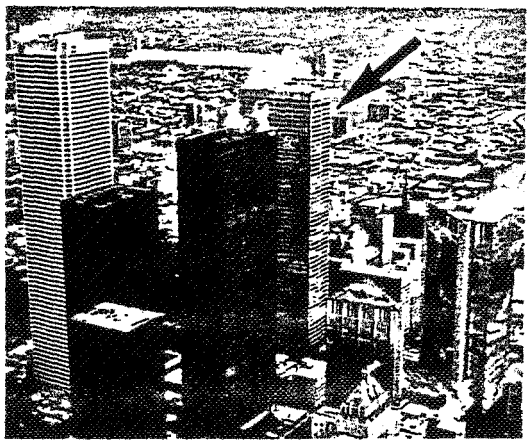

Figure 1 Commerce Court Tower (arrow) in downtown Toronto viewed from α=330°

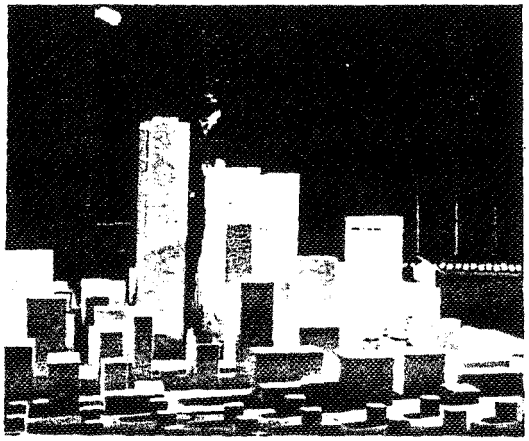

Figure 2 Commerce Court Model in NRC 9 m × 9 m Wind Tunnel viewed from α=10°

MODEL/FULL-SCALE BUILDING GEOMETRY

The 57-storey (239 m) Commerce Court Tower is situated in the core of Toronto and is surrounded on three sides by buildings of comparable height (Figure 1). The nearby tall buildings cover an area of 1 km^2; a strip of tall buildings, ½ km wide, extends several kilometres to the north. Surrounding these areas are several kilometres of relatively low buildings. Lake Ontario provides a smooth fetch beyond one kilometre to the south.

A 1:200 scale model of the Tower and its environs, including all adjacent tall buildings, was constructed (Figure 2). A power law profile of 0.33 was established outside the central core for approaches over the city from the west, north and east while a profile exponent of 0.15 was used for the lake exposure to the south. A third profile was provided for winds coming from near north by adding larger blocks to the urban roughness to simulate the strip of tall buildings. Each boundary layer was developed using spires at the inlet to the test section followed by roughness blocks. The detailed proximity model was mounted 18.3 m downstream of the spires on a 7.3 m diameter turntable.

MODEL-SCALE PRESSURE MEASUREMENTS

The mean and the root-mean-square-about-the-mean (rmsm) of the surface pressure fluctuations of the model as well as the associated minima and maxima were measured through a 360° wind direction range using increments of no greater than 10°. The Commerce Court pressure model had 96 surface pressure taps on four levels, 32 of which corresponded to locations on the full-scale building. Measurements were made with a calibrated pressure-tube-scanivalve-transducer system developed at the National Aeronautical Establishment[6], with a flat frequency response to 135 Hz. Each tap was sequentially sampled at 200 samples per second (200 s^{-1}) for 20 s.

The mean pressure coefficient is defined as

$$\overline{C_p} = \overline{(p - p_{ref})}/q = \bar{p}/q \qquad (1)$$

where the bar indicates an average over time, p is the measured pressure, p_{ref} is the reference static pressure and $q = \frac{1}{2}\rho\overline{v}^2$ is the reference dynamic pressure at the height of the anemometer location. (ρ is the density of air corrected for atmospheric temperature and pressure and $\overline{v}$ is the mean speed from the anemometer.) The rmsm surface pressure coefficient is

$$C_p' = \left[\overline{(p - \overline{p})^2}\right]^{\frac{1}{2}}/q = p'/q \qquad (2)$$

Time-series digital data from selected taps were recorded for several wind directions, at 500 s^{-1} for 200 s. These were used for the detailed studies of peak pressures.

FULL-SCALE PRESSURE MEASUREMENTS

The pressures were measured at 32 locations around the exterior of the building on four levels (Figure 3). Measurements were made relative to a common internal reference pressure. An anemometer and wind vane mounted on a mast on the roof 285 m above ground were used for the reference wind velocity measurements. The mean and rmsm of the full-scale pressure fluctuations, wind speeds and directions have been recorded for 5-min periods every hour for 6 years. Only the most recent 2 years of data (February 1976 to June 1978) are analyzed in this paper because new buildings were being erected in the vicinity prior to this period. Beginning in April 1977, maximum and minimum pressures were also recorded for each 5-min sampling interval. The signals were filtered with a 2-pole, 15 Hz low-pass filter and then sampled digitally at 20 s^{-1}. In addition to these summary data, time-series data sampled at 20 s^{-1} were recorded for longer periods during high winds.

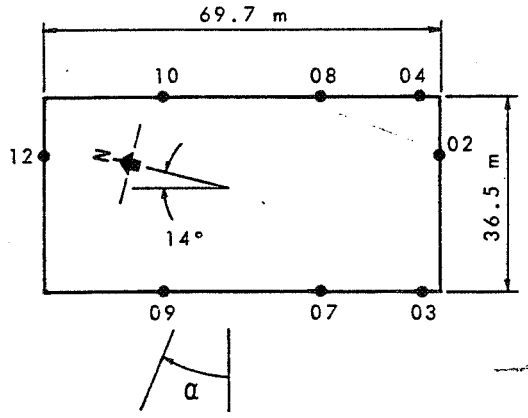

LEVEL	ELEV. m
ANEMOMETER	285
ROOF	239
3	202
4	166
5	138
7	102

e.g., TAP 304
3 - LEVEL
04 - TAP NUMBER

Figure 3 Location of pressure taps common to model and full-scale building

COMPARISON OF MEAN AND RMSM PRESSURES

Because full-scale pressures are affected not only by wind speed and direction, but also by the internal pressure due to building permeability, ventilation and temperature effects, a multiple linear regression must be performed to obtain mean pressure coefficients. The measured pressures are assumed to be described by

$$\overline{p} = \overline{p_o - p_i} = A + \overline{C_{pt}}\, q + \overline{C_T}\, p_b \left(\frac{1}{T_o} - \frac{1}{T_i}\right) \tag{3}$$

where p_o and p_i are outside and inside pressures respectively, p_b is barometric pressure, T_o and T_i are outside and inside absolute temperatures respectively and A, $\overline{C_{pt}}$ and $\overline{C_T}$ are coefficients determined by the least squares fit. The coefficient A represents the fixed pressure difference across the wall resulting from pressurization of the building with no wind and no temperature difference. The last term in the equation represents the pressure across the wall due to a temperature difference between inside and outside (stack effect). The wind pressure coefficient ($\overline{C_{pt}}$) represents the pressure difference that changes with wind velocity due to aerodynamic effects and can be represented by

$$\overline{C_{pt}} = \overline{C_p} - \overline{C_{pi}} \tag{4}$$

where $\overline{C_p}$ is the external pressure coefficient and $\overline{C_{pi}}$ is the mean internal pressure coefficient representing wind-induced variations in inside pressure due to building permeability.

A multiple linear regression performed on the mean pressure data reveals that the pressure is highly correlated with the stack effect so $\overline{C_T}$ has a large partial correlation coefficient ($r_{pT/q}$) typically greater than 0.85. On the other hand, the partial correlation coefficient ($r_{pq/T}$) of pressure with respect to dynamic reference pressure, q, ranges from 0.85 to 0.15 depending on wind direction. Large values of $r_{pq/T}$ are associated with relatively well-defined values of $\overline{C_{pt}}$; small values of $r_{pq/T}$ should be regarded as a warning that $\overline{C_{pt}}$ derived from that particular data set is unreliable.

The process of deriving $\overline{C_{pt}}$ from full-scale data is shown graphically in Figure 4. The line on each mean pressure plot (left side) has the equation $\overline{p} = A + \overline{C_{pt}}\, q$ so that A is the y-intercept and $\overline{C_{pt}}$ is the slope. Linear regression with dynamic pressure only provides rmsm pressure coefficients (C'_p) as slopes of the graphs on the right side of Figure 4. In general, the correlation coefficients (r_{pq}) for C'_p are greater than the partial correlation coefficients for $\overline{C_{pt}}$. The 225 data points plotted in Figures 4(a) and (b) were all obtained at nearly the same wind direction and extend to a maximum speed of 26 m/s. These features, particularly the wide wind-speed range, result in large values for $r_{pq/T}$ and, consequently, reliable estimates for $\overline{C_{pt}}$. Examples of data sets not possessing such desirable features are given in Figures 4(c) and (d); only 83 points were obtained within a 10° sector (253° to 263°) and, what is more important, there were no wind speeds over 12 m/s. Although a least-squares fit can always be derived, the low values of $r_{pq/T}$ indicate that little confidence should be placed in the slopes obtained. Another problem associated with low wind speeds in full-scale measurements is that thermal effects are more likely to produce a different flow than the neutral boundary layer simulated in the wind tunnel.

The difficulty in generating full-scale pressure coefficients to compare with wind tunnel results is illustrated by the scatter in Figure 4, for which there is no wind tunnel equivalent. In the wind tunnel, a mean pressure coefficient can be obtained at a fixed value of dynamic pressure and wind direction, with a repeatability of ±0.04 for $\overline{C_p}$ and ±0.01 for C'_p , even when the tests are performed one year apart. Much of this variation is due to minor differences in the model and boundary layer setup. If two runs of 20 s are made one after the other, the repeatability improves to ±0.01 and 0.005 for $\overline{C_p}$ and C'_p respectively.

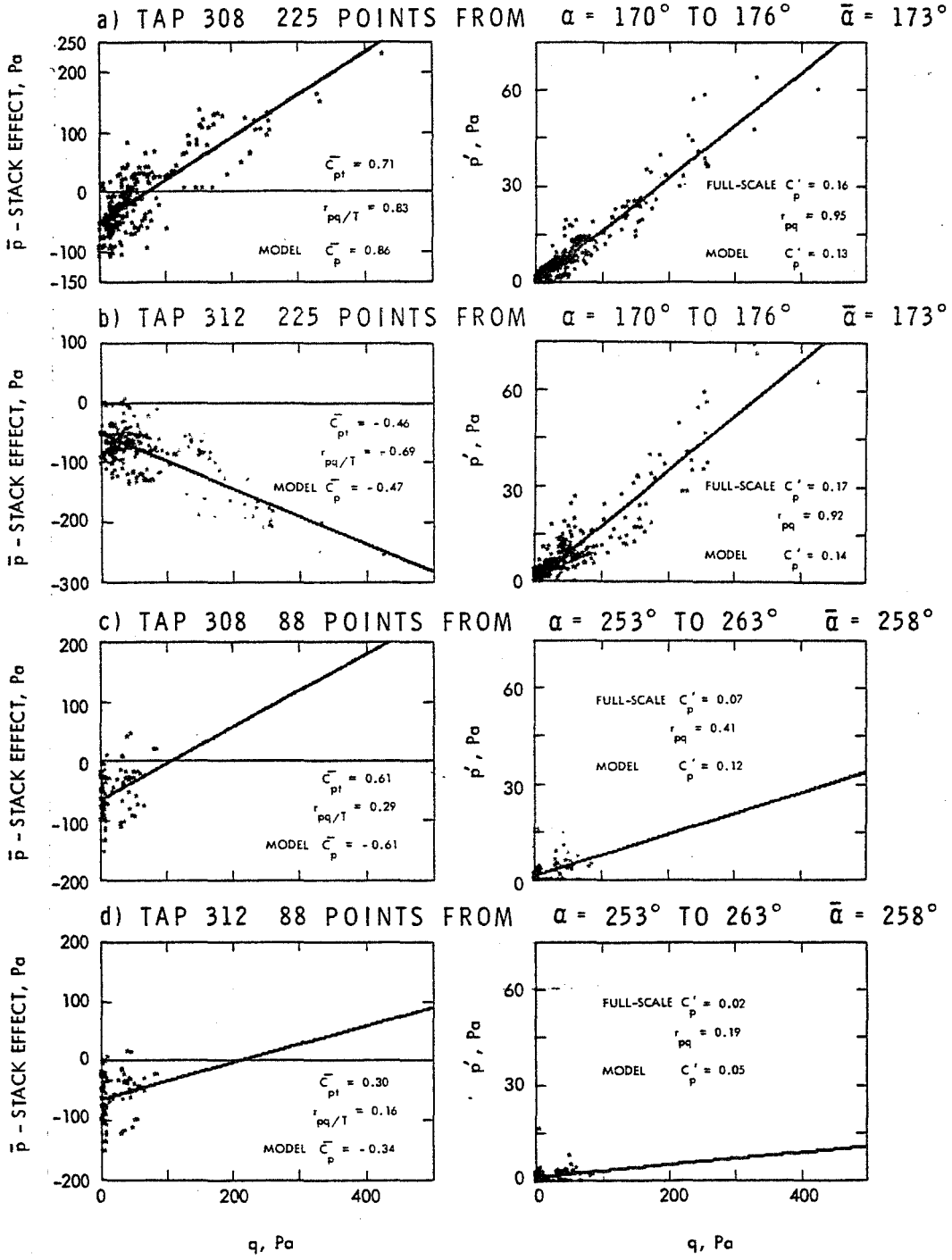

Figure 4 Measured full-scale surface pressures vs dynamic reference pressure

Since the pressures measured in full scale are differences between inside and outside, part of the scatter may be due to variations from hour to hour of the internal pressure due to building ventilation. Some of this effect was removed by dividing the data into day and night sets since the pressurization of the building is reduced at night, changing the values of A and $\overline{C_T}$. This also gave two independent sets of pressure coefficients.

$\overline{C_{pt}}$ coincides with $\overline{C_p}$ only if $\overline{C_{pi}}$ happens to be zero (Eq. 4); unfortunately, $\overline{C_{pi}}$ cannot be extracted using only the full-scale data. For any given wind direction, there should be a common offset between wind tunnel $\overline{C_p}$ and full-scale $\overline{C_{pt}}$ for the 32 pairs of corresponding taps, even though the offset will be somewhat obscured by random variations in the model/full-scale tap-pair differences. This common offset, taken to be the mean of the differences for the 32 tap-pairs, was removed from the results shown in Figure 5. The full-scale points in Figure 5(a) are offset upwards by a negligible amount, 0.01, but in Figure 5(b) the offset downwards is 0.67. Nevertheless, the remaining differences between wind tunnel and full scale are in each case roughly similar in character, with those of Figure 5(a) consistently smaller. In Figure 5(b) the south wall tap on level seven is the only tap for which comparison with wind tunnel results suffers badly because of the large offset. Taking all 51 wind sectors into account, the average offset is -0.12, not an unreasonable value for $\overline{C_{pi}}$ averaged over all wind directions. The authors have reservations, however, about equating these offsets to $\overline{C_{pi}}$. For some wind sectors with insufficient data and low partial correlation coefficients, the offsets give unlikely values for $\overline{C_{pi}}$. Even where the partial correlation coefficients are high, there remains an element of uncertainty in the comparisons of mean pressure coefficients because there was no independent evaluation of $\overline{C_{pi}}$. This is not a problem when comparing rmsm pressure

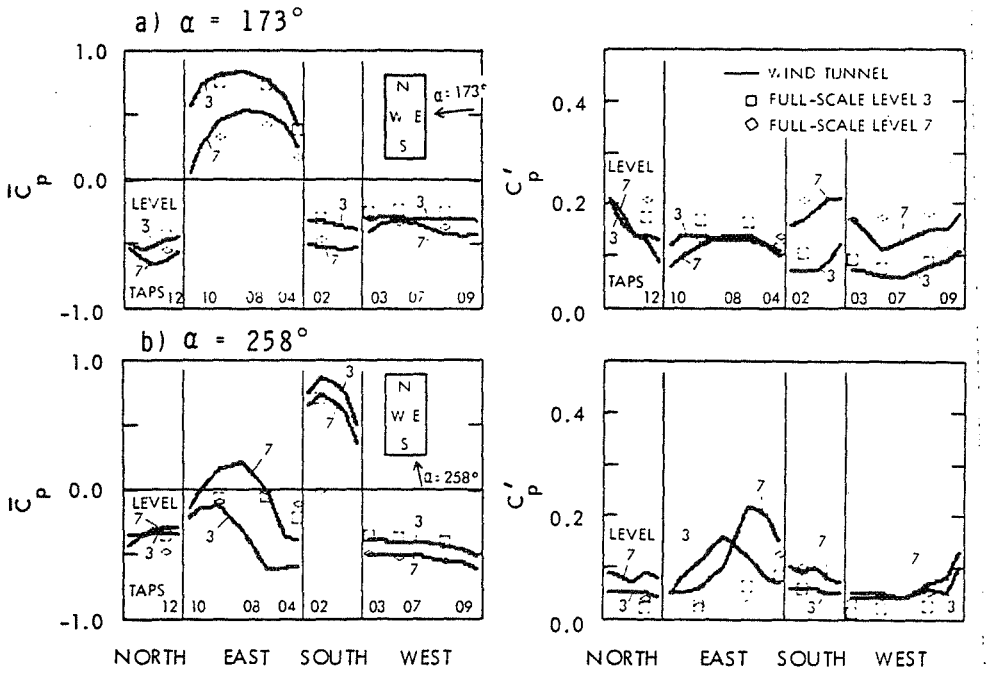

Figure 5 Level plots comparing model and full-scale pressures for two levels at 2 wind directions

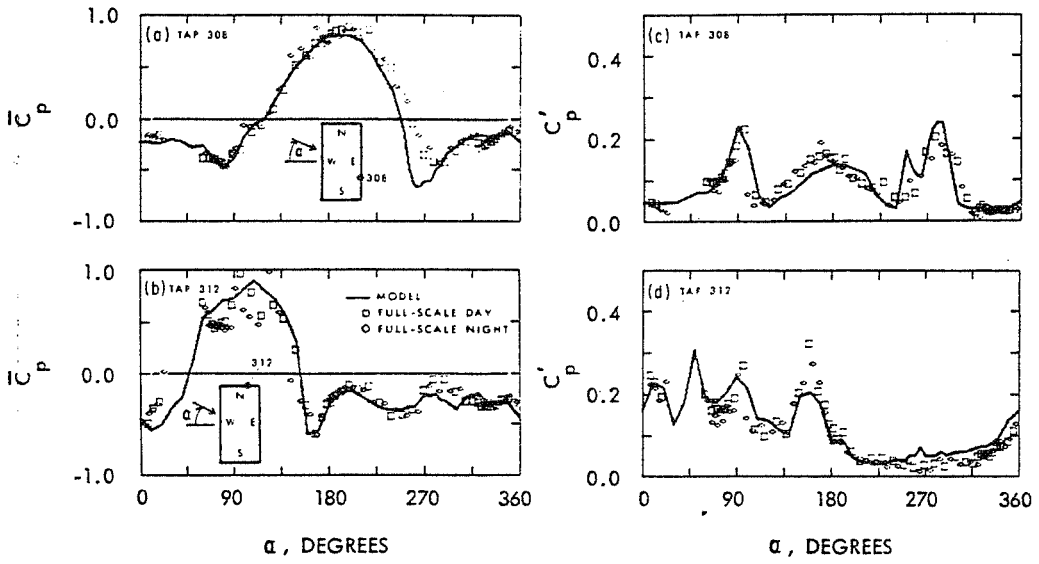

Figure 6 Pressure plots comparing model and full-scale results for two taps at all wind directions

coefficients because they are calculated on the same basis in wind tunnel and full-scale . Figure 6 shows general agreement between wind tunnel and full-scale pressure coefficients for two typical taps at all wind directions. The full-scale mean pressure coefficients (left) have the offset removed but the rmsm pressure coefficients (right) are directly from the linear regression.

PEAK PRESSURES

The peak pressure coefficient required for cladding design can be related to the mean and rmsm pressure coefficients by introducing a design peak factor, g_d:

$$C_{\hat{p}} = \overline{C_p} + g_d\, C'_p \tag{5}$$

The symbol $\hat{}$ denotes a positive extreme value; to simplify the discussion all peak factors will be treated as if positive. The assignment of a value for g_d is not as straightforward as for $\overline{C_p}$ and C'_p because the peak factor must account for the randomness inherent in pressure fluctuations. Although, for a given flow situation and building geometry, $\overline{C_p}$ and C'_p are nearly constant from one sampling interval to another, the maximum pressure observed will vary in a random fashion. A reasonable way of choosing a representative value for g_d might be to pick one of the following: the value that occurs most frequently (the mode), the average value (the mean), or the value with an acceptably small probability of being exceeded. Whatever the choice, information is required about the extreme value distribution of peak factors.

Peak factor parameters do not apply to the collection of values making up the sampling interval. Each sampling interval provides only one maximum; the extreme value distribution parameters apply to a collection of maxima derived from many such intervals. This does not mean that the statistics of the parent population of points in the sampling interval are unrelated to those of the extremes; on the

contrary, an expression for the extreme value distribution can be derived from the parent population. If the parent population is Gaussian, a type I double exponential distribution has been shown to apply to peaks[8] and for pressures on windward faces of a building reasonable agreement was found[4, 7]. In strongly turbulent negative pressure regions the tail of the parent population is much higher than the Gaussian, however, and predictions based on this assumption fall far short of observations.

PARENT POPULATION OF SPIKES

One solution to the difficulty of applying a Gaussian distribution to the points making up certain time records of fluctuating pressures is to say that intermittent "bursts" of turbulence are superimposed on a record that is otherwise Gaussian in nature. In other words, at random intervals throughout the sampling period, strong "spikes" of pressure occur, often with very short rise times. Because of their large values, all these spikes end up in the tail of the probability distribution and usually this is the only part of the distribution that is distinctly non-Gaussian. Of course, the tail of the distribution is the only part that is of interest for extreme value prediction.

This observation prompted a new line of investigation, aimed at the spikes rather than the entire population of points in the sampling interval. Two rules were devised, one to restrict consideration to events that would be significant from the standpoint of locating the extreme, and the second to ensure that the events were independent of one another. Each event is described by a single number called the spike value:

1) A spike value must be away from the mean by a threshold value at least twice the rmsm. Both mean and rmsm are measured over the entire sampling interval.

2) A spike must be separated from adjacent spikes by returns toward the mean that extend at least the threshold value from the spike value.

Figure 7 shows a short segment of record containing three spikes. The readings have been normalized by subtracting the mean value, then dividing by the rmsm value. Note that the second rule makes smaller "jiggles" in the record ineligible as spikes, even though they may be beyond the threshold level.

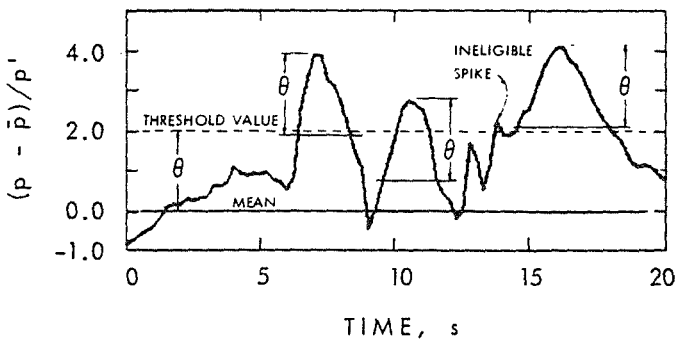

Figure 7 Typical time history with three spikes

The simplest distribution to apply to this new parent population, that of the spikes, is the negative exponential[9]. The cumulative distribution is:

$$F(g) = 1 - \exp\,[-(g - \theta)/(\bar{g} - \theta)] \tag{6}$$

The spike value g is normalized as $|p - \bar{p}|/p'$. θ is the threshold value, chosen to be 2, mentioned in the first rule, and $\bar{g}$ is the mean of the spike values in the interval. The extreme value distribution of peaks, $\hat{g}$, where each peak in the distribution is the maximum spike value from a sampling interval, is closely related to the above expression and requires only one more parameter:

$$F_n(\hat{g}) = \{1 - \exp\,[-(\hat{g} - \theta)/(\bar{g} - \theta)]\}^n \tag{7}$$

The new parameter n is the average number of spikes per interval. As one might expect, the longer the sampling interval, the larger the maximum spike value (peak). The value of the most probable peak (the mode $\tilde{g}$) increases linearly with the natural logarithm of n as follows:

$$\tilde{g} = (\bar{g} - \theta)\,\log_e n + \theta \tag{8}$$

For a proper comparison of peak pressures, the model sampling period must be the properly scaled equivalent of the full-scale period. The time scaling parameter is $\bar{t} = t\,\bar{v}/\ell$, where t and ℓ are a characteristic time and length. If t is chosen to be the sampling period (t_s) and ℓ is thought of as an average "spacing between spikes" (ℓ_s), then the average number of spikes per interval would be given by:

$$n = t_s\,\bar{v}/\ell_s \tag{9}$$

INVESTIGATION OF PRESSURE SPIKES AND PEAK FACTORS

Nine selected wind tunnel taps were sampled at 500 s^{-1} at a reference speed of $\bar{v}$ = 15 m/s to provide one hundred 2 s sampling intervals. Four histograms of pressure spikes were developed from groupings of two or three taps at a time using the two rules previously defined. The grouping was necessary to provide an acceptably large sample of peak factors.

One of the full-scale histograms was obtained by sampling eight pressure taps on the windward face of the building at 20 s^{-1} for 160 min when the wind had a direction of 350° and a mean speed of 23 m/s. This provided 256 5-min sampling intervals from which n and $\bar{g}$ could be established. The other three full-scale distributions were obtained from the peak values recorded for the hourly observations of 5-min periods sampled at 20 s^{-1} when the mean speed was, on average, 17 m/s. Histograms of peaks were fitted by extreme value distributions in order to obtain n and $\bar{g}$ for comparison with model scale. This method of "back-calculating" to determine n and $\bar{g}$ gave reasonable agreement when compared with directly measured values of n and $\bar{g}$.

Table 1 summarizes the exponential parameters found for both model and full scale. The histograms and the corresponding exponential curves are shown in Figures 8(a) to 8(d). Except for the three full-scale cases just mentioned, the exponential curves are defined by the observed values of n and $\bar{g}$ obtained from the time series

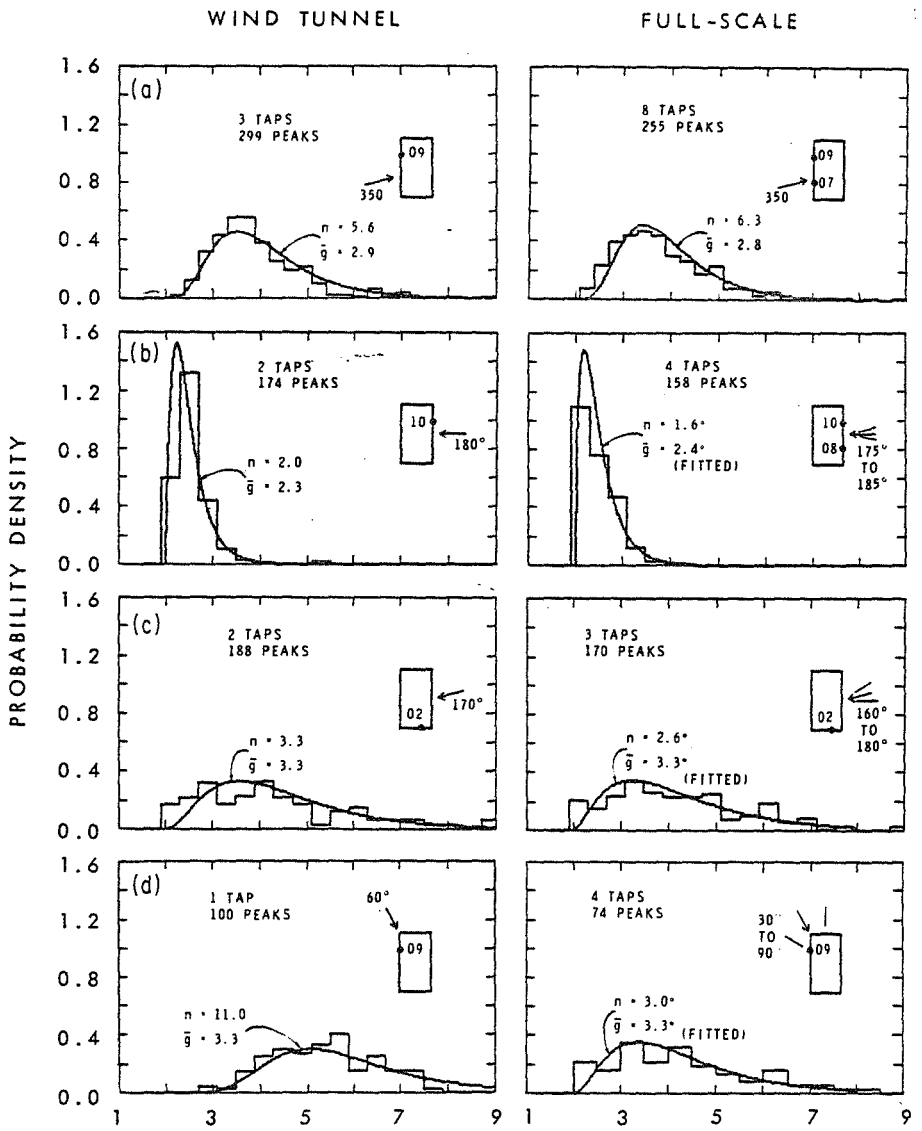

Figure 8 Peak pressure histograms and exponential curves

records defining the parent population of pressure spikes, and are not "fits" to the histograms. The fact that agreement is good even though most of the curves are derived from the parent population and not directly from the histograms of peaks indicates the usefulness of the concept of a parent population of spikes. Further, comparison of the model and full-scale distribution shows them to be in reasonable agreement, except for Figure 8(d) for which the model pressures were measured at a fixed wind direction of 60°, in the wake of a building 285 m high. To obtain sufficient data points at full scale for a histogram, data from a band between 30 and 90° had to be used, and even then only 74 points were found. Because of the localized variations of flow in a wake it is anticipated that the

Table 1. Properties of pressure spikes and peaks from wind tunnel and full scale

Item	Sign of Peak	F.S. Speed m/s	Parent Population (spikes)				Extreme Values (peaks)					
			n		$\bar{g}$		$\tilde{g}$		$\bar{\hat{g}}$		$\hat{g}'$	
			W.T.	F.S.	W.T.	F.S.	W.T.	F.S.	W.T.	F.S.	W.T.	F.S.
a	pos	23	5.6(6.4)	6.3	2.9	2.8	3.5	3.4	3.9	3.8	0.9	1.0
a'	pos	23		4.8		2.7		3.2		3.5		0.9
b	pos	17	2.0(1.7)	1.6*	2.3	2.4*	2.2	2.2	2.5	2.5	0.4	0.4
c	neg	17	3.3(2.8)	2.6*	3.3	3.3*	3.6	3.3	4.5	4.2	1.9	1.5
d	neg	17	11.0(9.4)	3.0*	3.3	3.3*	5.1	3.4	5.4	4.3	1.1	1.5

* no parent distribution available: n and $\bar{g}$ obtained from extreme value distribution fitted to match the mean and standard deviation, $\bar{\hat{g}}$ and $\hat{g}'$

( ) parentheses indicate wind tunnel values of n adjusted to represent a model sampling period equivalent to 5 min in full scale

unusual data at 60° in the wind tunnel would be masked in full scale by data from the rest of the sector.

Time scaling must be taken into account in a proper comparison of model and full-scale results. According to Eq. (9), values of n obtained from the 2 s records in the wind tunnel at a reference speed of 15 m/s correspond to those from the 5-min records in full scale only if the full-scale reference speed is 20 m/s, assuming the scale of mean "spike spacing" ℓ_s is the same as the geometric scale. Values of n adjusted to correspond to the full-scale 5-min record are shown in parentheses beside the measured wind tunnel values in Table 1.

Further investigation of the effects of time scaling indicates that sampling at 500 s^{-1} in the wind tunnel is equivalent to sampling at 3.8 s^{-1} for Item a (Table 1) and 2.8 s^{-1} for Items b to d. One might expect lower values at these lower model sampling rates compared to 20 s^{-1} which was used in full scale, but in fact the wind tunnel results are equal to or greater than the full scale in all but one case. The continuous record from full scale used for Item a was digitally filtered to simulate a single pole filter at 1.5 Hz and sampled at 4 s^{-1}. The properties of the filtered record, Item a', range from 4 to 10 percent below those for Item a except for n which dropped from 6.3 to 4.8. The filter characteristics of the model sampling system were not well represented by a single pole filter, however, and the half-power point was closer to 5 Hz (full scale) than to 1.5 Hz. In any case, filter characteristics and sampling rates of the measuring system evidently influence the magnitude of the pressure spikes recorded, and even larger effects may be seen in their shapes.

SLOPES OF PRESSURE SPIKES

Spikes come in a variety of shapes. Although on a compressed time scale they may look like vertical lines, on an expanded scale like that in Figure 7 they can often be roughly described as a triangular pulse with a base width (extended back to the mean level) varying from 1 to 10 s. The slopes of 29 of the largest spikes of the

full-scale records for Item a of Table 1 were found to average 7.3 C_p'/s with a coefficient of variation (c.c.v. = standard deviation ÷ mean value) of 0.7. On the other hand, 56 of the largest spikes from the wind tunnel study gave an average of 3.0 C_p'/s (c.o.v. = 0.6). The large discrepancy may be due to the differences in high frequency filtering and sampling rates. When the filtered full-scale record sampled at 4 s^{-1} was examined, the rate was found to be 2.7 C_p'/s (c.o.v. = 0.7). The slopes discussed so far have been for positive peaks; the average slope for 98 negative slopes from 19 tap locations sampled at 20 s^{-1} either in the wake or in glancing side-face flow was nearly double (14.2 C_p'/s with c.o.v. = 0.9). The full-scale slopes refer to a mean reference speed of 23 m/s, and would presumably be even steeper for higher speeds.

CONCLUDING REMARKS

The wind tunnel and full-scale mean and rmsm pressure coefficients agree well where there are sufficient full-scale data at high wind speeds. Wind speeds of at least 20 m/s are required to obtain reliable estimates of pressure coefficients for a particular wind direction at full scale. Otherwise, the full-scale data have too much random variation to be of use. Part of the pressure variation could be eliminated by obtaining a reference pressure independent of internal building pressure, as would be provided by a static pressure tap away from the influence of the building.

A scheme has been proposed for identifying significant independent peak events, pressure spikes, as they occur at random intervals in a time series, the statistical properties of which can be adequately described by an exponential distribution. Two parameters, the number of spikes in the interval and the average spike value, describe the extreme value distribution of peaks at a particular pressure tap or group of taps, allowing the peak at any desired probability level to be predicted for any storm duration. Positive pressure regions, for which positive peaks are of interest, typically have narrow probability density functions centred at peak factors lower than regions of positive pressure that are influenced by wakes. Negative pressure regions, particularly on side walls near upstream corners, exhibit broader distributions extending to larger peak factors than for positive pressures.

Considering the differences in the model and full-scale measuring systems, the agreement found between peak distribution parameters is encouraging. Additional experiments are planned in which greater attention will be paid to a proper matching of sampling rates and filter characteristics of wind tunnel and full-scale measuring systems. Changing the filter and sample rate for one full-scale record gave higher peaks for the larger rate, a trend that may continue even beyond 20 s^{-1}. In view of the difficulty and expense of raising sampling capabilities, it is worth examining the response of the cladding to peaks.

Annealed float glass office windows provide a particularly interesting example because their capacity to withstand peak pressures is thought to increase approximately as the 1/13th power of the peak slope[10]. This would mean that the 9 percent increase in peak magnitude ($\hat{g}$) at the higher sampling rate is almost matched by an 8 percent increase in capacity resulting from the increase in peak slope from 2.7 $C_p' s^{-1}$ to 7.3 $C_p' s^{-1}$. This example, although over-simplified and based on insufficient data, illustrates some of the considerations in assessing the adequacy of design data. Each cladding application may have somewhat different requirements, depending on material properties, size, and natural frequency. The need for more information on the response of cladding as well as the characteristics of the loading is apparent. Nevertheless, the

authors suggest that wind tunnel procedures of the sort described can provide adequate data for cladding design for high-rise buildings. Unless the effects of scale (sampling rate, sample length, reference speed) are accounted for, however, systematic peak prediction errors will result, and the practice of observing only a single peak to determine the design pressure coefficient will occasionally yield unrepresentative values. The authors recommend that peaks be selected from at least 10 subsets of an extended sampling interval, to permit "back-calculation" of n and $\overline{g}$ and a more soundly based prediction of peak pressure coefficients.

ACKNOWLEDGEMENTS

The authors wish to express their sincere appreciation to the following organizations and individuals for their contributions to this paper: Canadian Imperial Bank of Commerce, owners of the building; members of the Low Speed Aerodynamics Section, National Aeronautical Establishment; and colleagues, particularly P.J. Daly and F.W.K. Hummel, of the Division of Building Research. This paper is a joint contribution of two Divisions of the National Research Council of Canada: the National Aeronautical Establishment and the Division of Building Research. It is published with the approval of the Directors of these Divisions.

REFERENCES:

1. K.J. Eaton and J.R. Mayne, The measurement of wind pressures on two-storey houses at Aylesbury, J. Ind. Aerodynamics, 1, 67 (1975).

2. R.D. Marshall, A study of wind pressures on a single-family dwelling in model and full-scale, J. Ind. Aerodynamics, 1, 177 (1975).

3. W.A. Dalgliesh, Comparison of model/full-scale wind pressures on a high-rise building, J. Ind. Aerodynamics, 1, 55 (1975).

4. J.A. Peterka and J.E. Cermak, Wind pressures on buildings - probability densities, Proc. ASCE, Vol. 101, No. ST6, p. 1255-1267 (1975).

5. K.J. Eaton, Cladding and the wind, Proc. ASCE, Vol. 102, No. ST5, p. 1043-1058 (1976).

6. H.P.A.H. Irwin and K.R. Cooper, Correction of distortion effects caused by tubing systems in measurement of fluctuating pressures, National Research Council of Canada, LTR-LA-222 (1979).

7. W.A. Dalgliesh, Statistical treatment of peak gusts on cladding, Proc. ASCE, Vol. 97, No. ST9, September 1971, p. 2173-2187 (1971).

8. A.G. Davenport, Note on the distribution of the largest value of a random function with application to gust loading, Proc. Inst. Civ. Eng. 28, 187 (1964).

9. E.J. Gumbel, Statistics of extremes, Columbia University Press, New York, 1958, p. 113-118.

10. W.G. Brown, A load duration theory for glass design, National Research Council of Canada, Division of Building Research, Res. Paper 508 (1972).